



Research article

How does lake water clarity affect lake thermal processes?

Qunhui Zhang^{a,*}, Xiaogang Ma^b^a College of Tourism, Henan Normal University, Xinxiang 453007, Henan, China^b Department of Earth System Science, Ministry of Education Key Laboratory for Earth System Modeling, Institute for Global Change Studies, Tsinghua University, Beijing 100084, China

ARTICLE INFO

Keywords:

Lake water clarity
Lake model
Extinction coefficient
Lake thermal processes

ABSTRACT

The objective of this study was to determine the effects of water clarity changes on thermal processes in Lake Poyang, the largest freshwater lake in China, using a physically based lake model embedded in the Community Land Model. A water extinction coefficient (K_d) describing water clarity and controlling radiation penetration in the lake model was used to conduct controlled simulations. Three sets of simulations were conducted for Lake Poyang over the period from 2000 to 2015: DEFAULT with the $K_d = 0.45 \text{ m}^{-1}$; CTL with the $K_d = 1.68 \text{ m}^{-1}$ based on a water clarity of 0.85 m; and DARK with the $K_d = 1.68 \text{ m}^{-1}$ from 2000 to 2005 and $K_d = 3.44 \text{ m}^{-1}$ based on a water clarity of 0.41 m observed from 2005 to 2015. The simulation results showed that compared with the DEFAULT simulation, the temperature simulations were closer to the observations using the more accurate K_d values for the CTL and DARK simulations. Due to decreased water clarity, radiation absorbed in the top 1 m of the water body was larger for the DARK simulation and lower at greater depths than that observed for the CTL simulation. Such changes in radiation penetration in the DARK simulation generated a higher lake water surface temperature (LWST) and thus stronger lake-air interactions from February to July and lower LWST and turbulent fluxes from August to the following January than in the CTL simulation. The temperature inside the lake water body declined markedly, with a significant reduction from June to August that exceeded 5 °C. The results of this study provide an additional reference regarding lake water clarity effects on inland freshwater systems and theoretical support for lake water system management.

1. Introduction

Lakes around the world are sentinels and indicators of climate change (Adrian et al., 2009; Shimoda et al., 2011; Zhang and Duan, 2021). Lakes have a critical impact on local and regional climates, hydrology, and ecosystems mainly due to the unique properties of lakes such as larger heat content, lower albedo, and smaller roughness length than the surrounding land (widely known as “the lake effect”) (Thierry et al., 2015; Dai et al., 2018; Wu et al., 2019). Certain lake processes, such as increased lake water surface temperature (LWST), decreased lake ice cover, and enhanced lake stratification, have responded rapidly to global climate change (O'reilly et al., 2015; Woolway and Merchant, 2019; Yu et al., 2020). And these processes will likely continue to proceed in the future (Shatwell et al., 2019; Woolway et al., 2021; Grant et al., 2021). Hence, exploring lake processes and their responses to changes in climate and the environment contributes to studies on climate, hydrology, and ecological systems.

Water clarity is a key factor representing lake water quality, and it impacts the physical and ecological processes in lakes (McPherson et al., 2011; McCullough et al., 2012; Olmanson et al., 2013). Water clarity is affected by substances within lake water, primarily aquatic plankton, suspended particles, and dissolved organic matter (Aas et al., 2014; Shang et al., 2016). With the increasing availability of in situ observations and remote sensing data, researchers have carried out detailed studies on spatiotemporal distributions, changes, and the causes of lake water clarity at both single-lake and regional scales (Wang S et al., 2020; Bukaveckas et al., 2021; He et al., 2022).

Lake models are important tools for exploring lake thermal processes (Samuelsson et al., 2010; Huang et al., 2019; Lv et al., 2019). Water clarity is usually measured as the Secchi disk depth (SDD, m), and is generally quantified in lake models using an extinction coefficient (K_d) parameterized in the radiation penetration scheme (Bonan, 1995). The K_d is often set to a constant value or as a function of lake depth in lake models, dominating solar radiation transfer within the lake water body (Hakanson, 1995; Mironov, 2008; Stepanenko et al., 2012). Previous

* Corresponding author.

E-mail address: qunhui_zhang321@163.com (Q. Zhang).

numerical modeling work has shown that this parameter plays an important role in lake temperature simulations (Potes et al., 2012; Xu et al., 2016). Although only limited measured data exist for the K_d , with lake-specific and time-independent constant values, this parameter can be satisfactorily used for current lake modeling (Heiskanen et al., 2015).

To investigate the effect of lake water clarity changes on lake thermal structure, researchers have often used different K_d values for lake models to carry out controlled and sensitive experiments (Rinke et al., 2010; Potes et al., 2012). These previous research indicated that lake water clarity affected lake thermal processes through controlling radiation transfer within the lake (Hocking and Straškraba, 1999; Heiskanen et al., 2015). However, these work generally employed sensitive tests, and rare studies were conducted based on reality conditions with lakes that indeed have undergone water clarity changes.

In this study, we studied Lake Poyang, the largest freshwater lake in China, to explore the effect of the observed decreased water clarity from the late 1990s to the early 21st century. The one-dimensional lake scheme embedded in the Community Land Model (CLM_Lake) widely used in lake studies were employed (Oleson et al., 2013). Variables including LWST, water temperature profiles, and heat fluxes were analyzed to quantify the water clarity change effects on lake thermal processes. This studied lake, data, and CLM_Lake model are introduced in Section 2. Section 3 presents the simulation results and discussion, and the conclusions are given in Section 4.

2. Studied Lake, Data, and Model Setup

2.1. Studied lake

Lake Poyang, located at 28°11'–29°51' N, 115°49'–116°46' E (Figure 1), is the largest freshwater lake in China and is an important wetland in the world. This lake has longitudinal and lateral lengths of 170 km and 16.7 km, respectively. Lake Poyang has a subtropical monsoon climate with an average annual air temperature and precipitation of ~17 °C and ~1542 mm, respectively (Qi et al., 2018). The sources of water for this lake are mainly precipitation, rivers, and ground recharge (Li et al., 2020). Lake Poyang plays an essential role in supplying water and fishery resources for surrounding cities (Shankman

et al., 2006; Zhen et al., 2011; Wu et al., 2017). Water clarity for this lake has reportedly declined over time, and therefore, aquatic production and biodiversity have likely been affected (Zhang et al., 2020). However, how water clarity changes affect water thermal processes still remains unclear.

2.2. Data

The China Meteorological Forcing Dataset (CMFD) was used to drive the CLM_Lake model in this study. This dataset originated from remote sensing products, reanalysis datasets, and in situ observations (He et al., 2020) and has been widely applied in land process modeling and climate studies as meteorological observations because of its high accuracy (Chen et al., 2011; Zhu et al., 2020; Tian et al., 2020). The variables for the lake model included downward shortwave and long-wave radiation, air temperature, air pressure, wind speed, and specific humidity. These forcing data had a time-step of 3 h and a spatial resolution of $0.1^\circ \times 0.1^\circ$ and covered the period of 2000–2015 for this study. The monthly Moderate Resolution Imaging Spectroradiometer (MODIS) land surface temperature products with a 0.05° spatial resolution were used to evaluate the LWST simulation results. Previous research has proven that these MODIS products have acceptable accuracy compared with in situ observations for investigating lake thermal processes (Zhang et al., 2014).

Water clarity data for Lake Poyang were based on in situ observations from national investigations and a literature dataset (Zhang et al., 2020). Water clarity for Lake Poyang has declined over time, with a value of 0.85 m before 1995, and it has decreased to 0.41 m since 2005. We determined that these data were sufficient to conduct numerical modeling using CLM_Lake, which would further clarify the mechanism involved in how changes in water clarity affect thermal processes for this lake.

2.3. Model setup

The CLM_Lake model was used to investigate the water clarity change effect on lake thermal processes for Lake Poyang. This model has been applied extensively and has been combined with several regional climate models to study lake thermal processes and lake-air interactions (Thiery et al., 2014; Zhang et al., 2019; Wang et al., 2020). The lake model simulates lake thermal processes, including lake-air heat exchange, water mixing, and radiation penetration within lake water (Oleson et al., 2013; Subin et al., 2012). Lake temperatures are calculated using Eq. (1), an governing thermal diffusion equation:

$$\frac{\partial T}{\partial t} = \frac{\partial}{\partial z} \left(K_w \frac{\partial T}{\partial z} \right) + \frac{1}{C_w} \frac{\partial \phi}{\partial z} \quad (1)$$

where T is the lake temperature (K) at the lake depth of z (m) and time t (s), z is increasing downward, K_w is the total water diffusivity ($\text{m}^2 \text{s}^{-1}$), C_w is the volumetric heat capacity ($\text{J m}^{-3} \text{K}^{-1}$), and ϕ is the absorbed downward radiation flux as the heat source term (W m^{-2}).

The radiation penetration scheme separately estimates the radiation flux absorbed within various water layers, i.e., the upper water layer and the lower layer (Eq. (2)). For unfrozen lakes, the surface absorption fraction β (typically 0.5) is set according to the near-infrared radiation absorbed within the top z_a (set to 0.6 m in the model), and the remaining absorbed radiation fraction $(1 - \beta)$ within the lake water body is determined according to the Beer-Lambert Law. This was a simplification assuming exponential attenuation of light with lake water depth:

$$\phi = (1 - \beta) S_g \exp[-K_d(z - z_a)], \quad z > z_a \quad (2)$$

where ϕ (W m^{-2}) is the solar radiation remaining at a depth of z (m), β is the surface absorption fraction within the top z_a (0.6 m), S_g is the absorbed solar radiation in the lake, and K_d (m^{-1}) is a constant extinction coefficient as a function of lake depth:

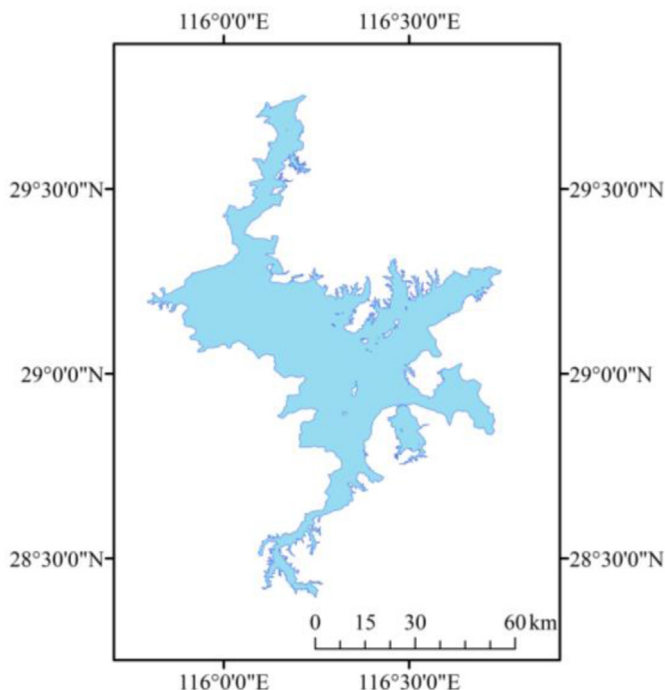


Figure 1. The location of Lake Poyang.

$$K_d = 1.1925D^{-0.424} \tag{3}$$

where D is the lake depth (m). Eq. (3) is from Hakanson (1995) based on statistics with observed data for K_d and water depth for 88 lakes.

In this study, the lake depth was set to a water mean depth of 10 m according to observations (Zhao et al., 2019). Based on this depth and Eq. (2), K_d was equal to 0.45 m^{-1} . Therefore, the default simulation (referred to as DEFAULT) had K_d set to 0.45 m^{-1} with a 0.1° horizontal resolution for Lake Poyang during the period of 2000–2015. Two other sets of simulations were carried out with model settings that were the same as the DEFAULT simulation, but with different K_d values. For the first five years (2000–2004), these two sets of simulations were conducted with K_d of 1.68 m^{-1} according to the numerical relationship with a water clarity of 0.85 m (Zhang et al., 2020). Then, in 2005, one simulation set maintained the K_d at 1.68 (referred to as CTL), but the other simulation set the K_d to 3.44 m^{-1} , corresponding to a lower water clarity of 0.41 m (referred to as DARK).

Simulations for the first five years (2000–2004) were discarded as they were regarded as the simulation initialization. The remaining simulations during 2005–2015 were used to evaluate differences between these three simulation results. In addition, we employed statistical metrics in this study, including the root mean square error (RMSE) and Pearson correlation coefficient (COR), for model evaluation.

3. Results

3.1. Model evaluation

Three simulations of LWST with the DEFAULT, CTL, and DARK model settings were compared to the MODIS products (Figure 2). All three simulations had high CORs (>0.9) with the MODIS observations, implying that CLM_Lake can generate reasonable seasonal and interannual temperature characteristics for Lake Poyang (Table 1). The DEFAULT simulations with the default extinction coefficient produced the largest RMSE. The CTL and DARK simulations produced LWST RMSEs

Table 1. Comparisons of lake water surface temperature (LWST) between simulations and MODIS observations using Pearson correlation coefficients (COR) and root mean square error (RMSE, °C).

	DEFAULT	CTL	DARK
COR	0.97	0.98	0.98
RMSE	5.0	4.2	3.8

that were 0.8°C and 1.2°C lower, respectively, than the RMSE of the DEFAULT simulation. In addition, DARK simulation performed the best with the highest correlation coefficient and the smallest RMSE. Thus, more accurate water extinction coefficients set in the lake model simulated the LWST more close to observations.

3.2. The effect of water clarity changes on lake thermal processes

The effect of water clarity changes on lake thermal structure can be clarified by comparing the CTL and DARK simulations. Figure 3 shows the radiation penetration simulations for these two simulations with monthly and annual average results for 11 years during 2005–2015. Decreased water clarity with the DARK simulation caused more solar radiation to be absorbed in the top of the water body than with the CTL simulation. As mentioned in Section 2.2, surface radiation absorption within the surface 0.6 m was unchanged, while below this depth and around the depth of 1 m , more radiation was absorbed with the DARK simulation than with the CTL simulation, with the maximum difference of 8 W m^{-2} occurring in July. In the upper part of the water profile, there was a more rapid decline in absorbed radiation with the DARK simulation than with CTL simulation, with the most significant reduction by 14 W m^{-2} occurring in July (Figure 3a).

As seen for the multiyear average, the largest increase in absorption (4 W m^{-2}) occurred in the surface layers, accounting for 13% more absorption with the DARK simulation than with the CTL simulation. The largest reduction occurred inside the lake with 8 W m^{-2} (Figure 3b-c).

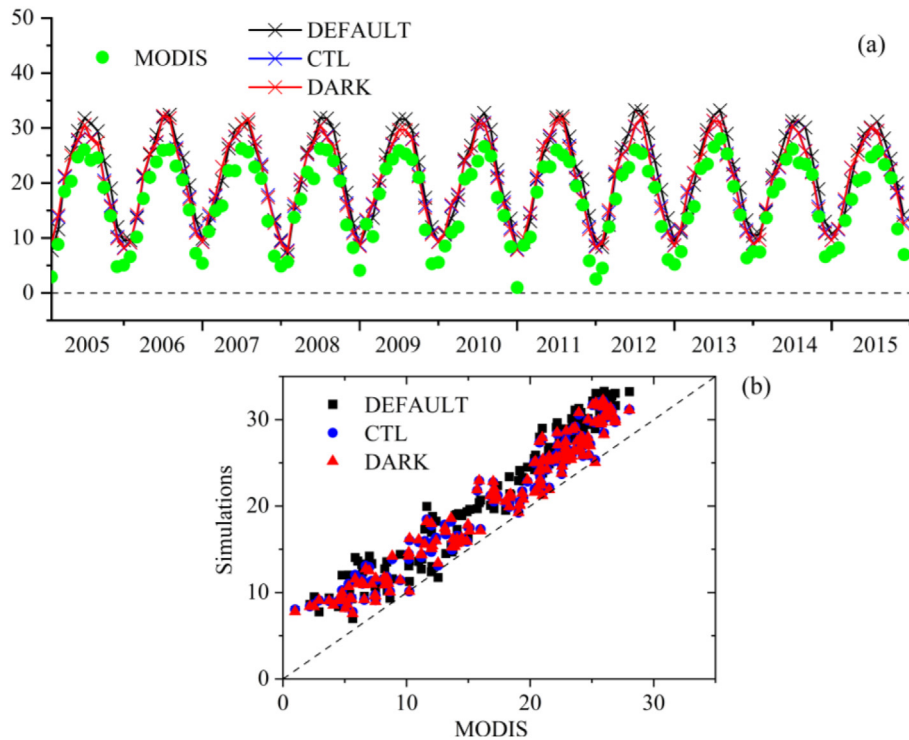


Figure 2. (a) Lake water surface temperature (LWST, °C) observations for Lake Poyang from MODIS (green circles) and simulations with the DEFAULT (black line), CTL (blue line), and DARK simulations (red line). (b) Comparisons between simulations from DEFAULT, CTL, and DARK and MODIS (y represents MODIS, and x represents simulations).

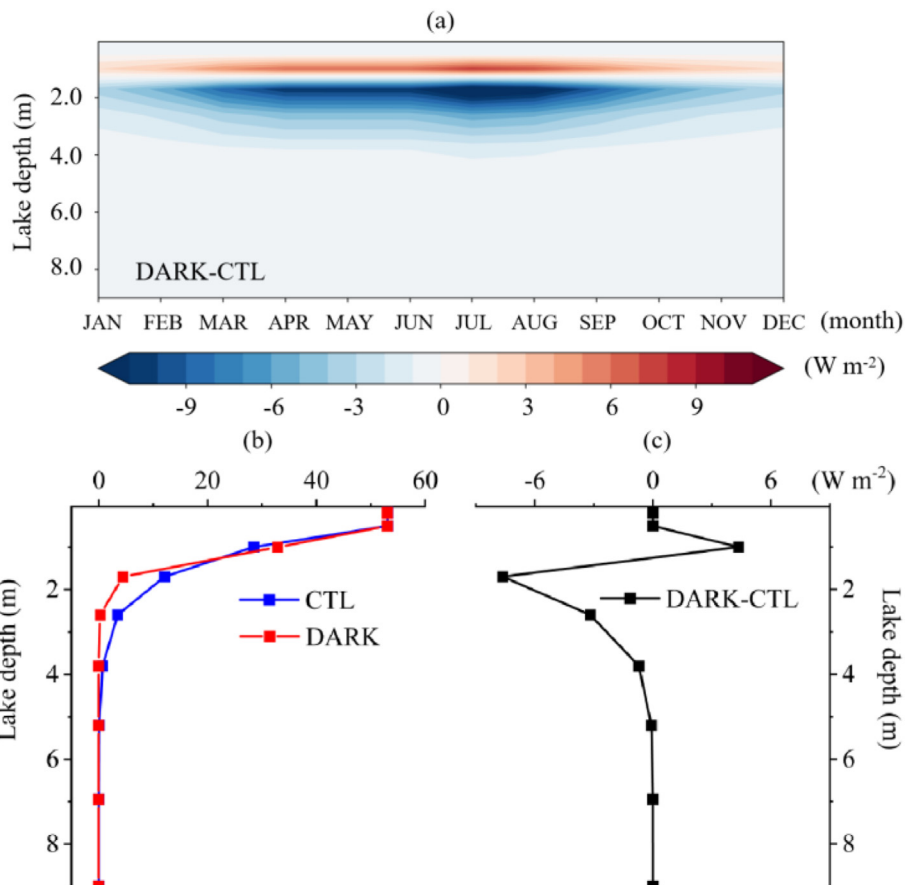


Figure 3. Simulated solar radiation absorbed ($W m^{-2}$) within the Lake Poyang water. (a) Differences in monthly averages between DARK and CTL; (b) multiannual averages of DARK and CTL and (c) multiannual differences (DARK-CTL).

Such differences in radiation absorption within the lake water body between the CTL and DARK simulations would cause changes in the lake thermal processes.

The thermal process differences averaged for the period of 2005–2015 between the CTL and DARK simulations were analyzed. Simulated LWST differences for the lake are shown with multiyear monthly averages in Figure 4. The lake water clarity was reduced in the DARK simulation compared with the increased LWST in the CTL simulation from February to July and reduced LWST from August to the following January (Figure 4). The maximum increase and decrease in LWST due to water clarity occurred in March and November, with values

of 0.3 °C and -0.35 °C, respectively. The multiannual average of LWST from the CTL to DARK simulations decreased by approximately 0.05 °C. In addition, the seasonal variation range for the DARK simulation was 0.2 °C larger than that in the CTL simulation. Such changes in LWST caused by lake water clarity changes were related to the lake energy budget (analyzed below).

Heat fluxes simulated with CTL and DARK, including sensible heat fluxes (SH), latent heat fluxes (LH), and net ground heat stored (G), were also compared (Figure 5). Due to more radiation absorbed in the top water layers with DARK, the increased LWST from February to July

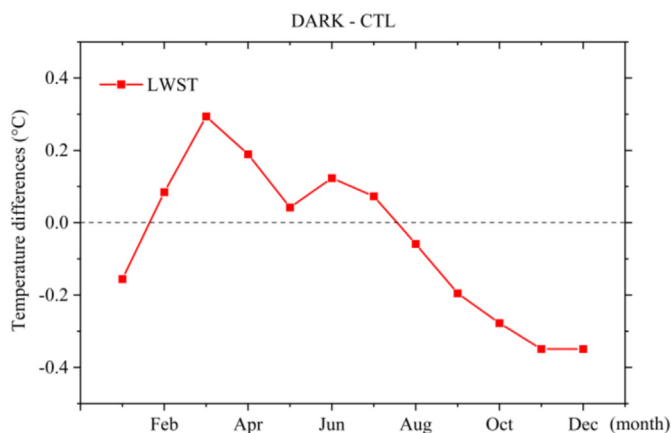


Figure 4. Lake water surface temperature (LWST, °C) differences between simulations with DARK and CTL (DARK-CTL) for Lake Poyang.

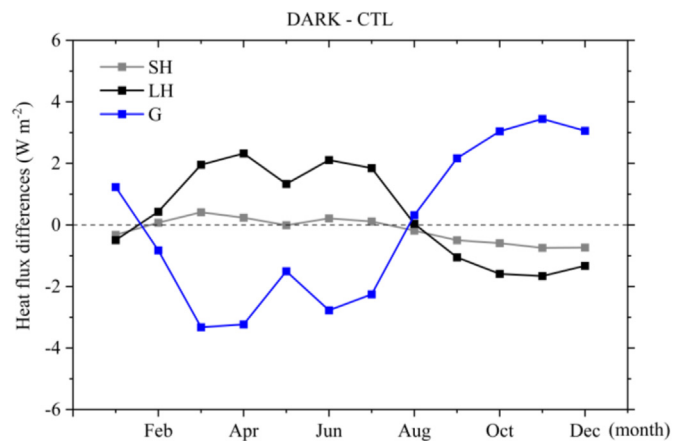


Figure 5. Heat flux differences ($W m^{-2}$) for sensible heat flux (SH, gray line) and latent heat flux (LH, black line), and net ground heat stored (G, blue line) from simulations between DARK and CTL (DARK-CTL) for Lake Poyang.

enhanced the water and heat exchanges between the lake surface and the atmosphere, increasing the heat fluxes of SH and LH. These increased heat fluxes released from the lake led to less heat being stored in the lake water, with a maximum heat content G of $\sim 3 \text{ W m}^{-2}$ in March. The lower heat storage with DARK compared with CTL caused a rapid cooling of LWST, thus lessening the lake-air interactions with decreased SH and LH and increasing heat storage of G during August to the following January. And the increased heat storage reached to $\sim 3 \text{ W m}^{-2}$ in November.

These seasonal changes caused the annual average LH increased by 3% in DARK compared to that in CTL, while the SH changed little. In addition, the worse water clarity with DARK decreased the annual average heat stored within the lake by 25%. Such seasonal and annual thermal changes may weaken the lake effect, which is known to have a larger heat content than the surrounding land.

Monthly lake water temperature profiles averaged for 11 years during 2005–2015 for the CTL and DARK simulations were further compared to quantify the effect of water clarity changes on thermal processes in the lake water interior. Due to more radiation being absorbed in the top water layers and less being absorbed at greater lake depths, the water temperature of the surface layers (at a depth of 0–1 m) was slightly greater for the DARK simulation than for the CTL simulation from February to July, which was during the same period of greater LWST, as shown in Figure 4. Below the surface layers, the water temperature decreased overall due to less radiation being absorbed, with the maximum reduction exceeding 5°C in summer (from June to August) at a depth of 2–4 m (Figure 6). Afterward, these marked changes in the thermal structure with a lower water clarity in the DARK simulation reduced the temperature gradient within the lake water, especially in warm seasons, thereby enhancing water stability and lowering the likelihood of water turnover inside the lake. Diminished water turnover negatively impacts aquatic life and lake ecosystems.

The aforementioned results from this study were consistent with previous research (Heiskanen et al., 2015; Zolfaghari et al., 2017). Water clarity affected solar radiation penetration and distribution within the lake, thereby influencing LWST and lake-air interactions. Changes in energy allocation changed the heat content within the lake, in turn changing the LWST and lake temperature profiles. Finally, more turbid lake water had lower water temperature profiles and larger LWST seasonal variations, resulting in decreased heat content within the lake water body. This analysis indicated that ecological changes in lake water clarity would have a nonnegligible impact on water thermal processes.

3.3. Discussion

3.3.1. Calculation of the extinction coefficient in lake models

The results from this study suggested that significant changes in lake water clarity should not be ignored in lake process simulation research. However, most current one-dimensional lake models with fixed or unrealistic K_d values do not adequately represent water clarity changes. For example, the K_d is set to constant values in the well-known FLake (Mironov, 2008) and LAKE (Stepanenko et al., 2012) models. Other models embedded in the lake-air coupled Weather Research and Forecasting (WRF) model (Gu et al., 2013), the Common Land Model (CoLM) (Dai et al., 2003), and the CLM used in this study described K_d as a function of lake depth (see Eq. (3)). There are also some lake models that calculate the K_d using lake water biomass, while these models have a high demand for observed lake data (Goudsmit et al., 2002).

Currently such above lake models cannot present dynamic lake water clarity changes, and simply inputting observed K_d values into lake models cannot satisfy the simulation needs of lake-rich areas. Hence, future modeling research should be directed at further improving and renewing the radiation penetration scheme by considering dynamic lake water clarity changes, especially for lakes with remarkable lake ecological changes.

Presently, there is a lack of global lake extinction coefficient datasets because of temporal and spatial discontinuity problems. As optical remote sensing technology develops, water clarity data will gradually become more plentiful and accessible, and these datasets should be validated using in situ observations. The relationship between the SDD and K_d varies for lakes in different regions (Padial and Thomaz, 2008; Zhang et al., 2012). Such relationships are currently of three general types, including inverse proportional, modified inverse proportional, and power function relationships based on lake-specific data (Poole and Atkins, 1929; Bukata et al., 1998; Zhang et al., 2020). To express water clarity changes in lake modeling, the relationship between these two parameters can be utilized to investigate thermal responses to lake ecology changes. In addition, next-generation remote sensing data verified with in situ observations of lake water clarity can also be applied and imported into lake process simulations, further effectively deepening the understanding of coupled physical and ecological processes for lakes.

3.3.2. Limitations

We recognize that several limitations exist in our study. First, in situ observations of water clarity for Lake Poyang were interdecadal. Although the mechanism of the water clarity change effect on lake

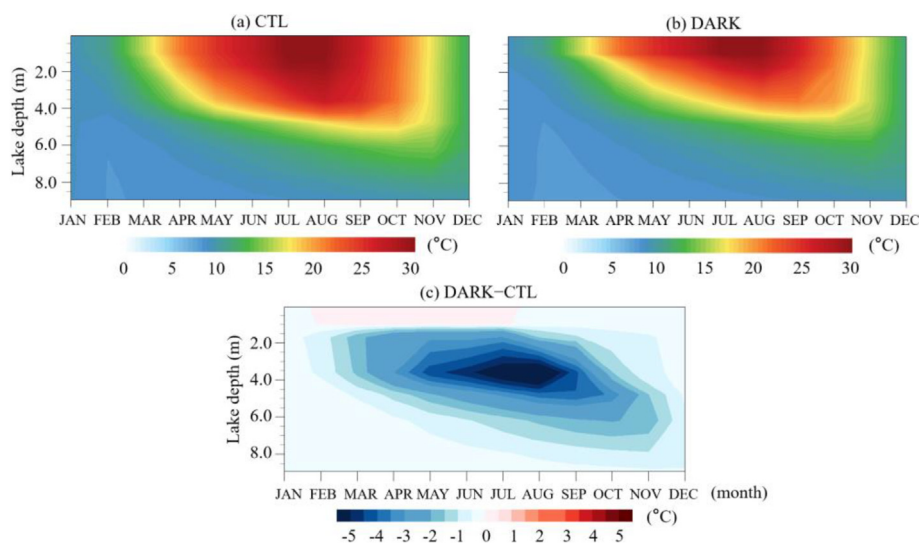


Figure 6. Lake temperature ($^{\circ}\text{C}$) profile simulations for Lake Poyang from (a) CTL and (b) DARK; (c) differences between DARK and CRL (DARK-CTL).

thermal processes could be determined based on these data, lake water clarity data with higher precision (regarding both time step and spatial resolution) are needed in the future to conduct lake ecology and physical process research. Second, the results of this study showed that lake water clarity changes could result in obvious thermal changes within a lake that should not be ignored. Such thermal responses could lead to changes in lake ice phenology for frozen lakes such as lakes in the Tibetan Plateau and the Arctic. Lake Poyang rarely freezes, but more attention should be given to lake thermal processes responding to lake water clarity for northern or high-altitude lakes. Last, we did not consider or discuss whether the lake effect on local and regional climate was influenced by water clarity changes. Hence, future research should explore local or regional responses to significant lake water clarity changes.

4. Conclusions

In this study, we carried out a modeling study for Lake Poyang using the CLM_Lake model to investigate the water clarity change effect on lake thermal processes. Three simulations including DEFAULT, CTL, and DARK were conducted during 2000–2015 using the radiation penetration factor of the water extinction coefficient K_d to represent water clarity changes. The results showed that the more accurate K_d values used by the DARK and CTL simulations produced LWST values closer to the observations derived from the MODIS data than the LWST simulated by DEFAULT. The DARK simulation with a lower water clarity had more radiation absorption in the top lake layers and less absorption at greater depths than that in the CTL simulation. Such a change in the DARK simulation increased the LWST from February to July, enhanced the lake-air interaction, and reduced the heat stored within the lake. This caused a rapid decline in the LWST from August to the following January, further weakening the lake-air interactions. In addition, due to the reduced radiation absorbed at greater depths, the water temperature decreased significantly especially from June to August, with the maximum reduction exceeding 5 °C in the DARK simulation when compared to the CTL simulation. This study provides additional evidence of the probable thermal responses from changes in lake ecology factors that may improve investigations of inland freshwater ecology, hydrology, and climate systems.

Declarations

Author contribution statement

Qunhui Zhang: Conceived and designed the experiments; Performed the experiments; Analyzed and interpreted the data; Wrote the paper.
Xiaogang Ma: Wrote the paper.

Funding statement

Ms Qunhui Zhang was supported by Doctoral Scientific Research Foundation of Henan Normal University [QD2021091].

Data availability statement

Data will be made available on request.

Declaration of interest's statement

The authors declare no conflict of interest.

Additional information

No additional information is available for this paper.

Acknowledgements

The China Meteorological Forcing Dataset used in this study as forcing data was accessible from the Third Pole Environment Database (<http://data.tpdc.ac.cn/zh-hans/data/8028b944-daaa-4511-8769-965612652c49>, last accessed: 29 March 2022). The MODIS land temperature data products (MOD11 and MYD11) were from <https://modis.gsfc.nasa.gov/data/dataproduct> (last accessed: 29 March 2022).

References

- Aas, E., Høkedal, J., Sørensen, K., 2014. Secchi depth in the Oslofjord-Skagerrak area: theory, experiments and relationships to other quantities. *Ocean Sci.* 10 (2), 177–199.
- Adrian, R., O'Reilly, C.M., Zagarese, H., Baines, S.B., Hessen, D.O., Keller, W., Livingstone, D.M., Sommaruga, R., Straile, D., Van Donk, E., Weyhenmeyer, G.A., Winder, M., 2009. Lakes as sentinels of climate change. *Limnol. Oceanogr.* 54 (6), 2283–2297.
- Bonan, G.B., 1995. Sensitivity of a GCM simulation to inclusion of inland water surfaces. *J. Clim.* 8 (11), 2691–2704.
- Bukaveckas, P.A., 2021. Changes in acidity, DOC, and water clarity of Adirondack lakes over a 30-year span. *Aquat. Sci.* 83, 50.
- Bukata, R.P., Jerome, J.H., Bruton, J.E., 1998. Relationships among secchi disk depth, beam attenuation coefficient, and irradiance attenuation coefficient for great lakes waters. *J. Great Lake Res.* 14 (3), 347–355.
- Chen, Y., Yang, K., He, J., Qin, J., Shi, J., Du, J., He, Q., 2011. Improving land surface temperature modeling for dry land of China. *J. Geophys. Res.* 116, D20104.
- Dai, Y., Wang, L., Yao, T., Li, X., Zhu, L., Zhang, X., 2018. Observed and simulated lake effect precipitation over the Tibetan plateau: an initial study at nam Co lake. *J. Geophys. Res. Atmos.* 123 (13), 6746–6759.
- Dai, Y.J., Zeng, X.B., Dickinson, R.E., Baker, L., Bonan, G.B., Bosilovich, M.G., Denning, A.S., Dirmeyer, P.A., Houser, P.R., Niu, G.Y., Oleson, K.W., Schlosser, C.A., Yang, Z.L., 2003. The Common land model. *Bull. Am. Meteorol. Soc.* 84 (8), 1013–1023.
- Goudsmit, G.H., Burchard, H., Peeters, F., Wüest, A., 2002. Application of k-ε turbulence models to enclosed basins: the role of internal seiches. *J. Geophys. Res. Atmos.* 107 (12), 3230.
- Grant, L., Vanderkelen, I., Gudmundsson, L., Tan, Z., Perroud, M., Stepanenko, V.M., Debolskiy, A.V., Droppers, B., Janssen, A.B.G., Woolway, R.L., Choulga, M., Balsamo, G., Kirillin, G., Schewe, J., Zhao, F., Vega, I., Golub, M., Pierson, D., Marcé, R., Seneviratne, S.I., Thiery, W., 2021. Attribution of global lake systems change to anthropogenic forcing. *Nat. Geosci.* 14, 849–854.
- Gu, H., Jin, J., Wu, Y., Ek, M.B., Subin, Z.M., 2013. Calibration and validation of lake surface temperature simulations with the coupled WRF-lake model. *Climatic Change* 129 (3–4), 471–483.
- Hakanson, L., 1995. Models to predict Secchi depth in small glacial lakes. *Aquat. Sci.* 57 (1), 31–53.
- He, J., Yang, K., Tang, W., Lu, H., Qin, J., Chen, Y., Li, X., 2020. The first high resolution meteorological forcing dataset for land process studies over China. *Sci. Data* 7 (25), 1–7.
- He, Y., Lu, Z., Wang, W., Zhang, D., Zhang, Y., Qin, B., Shi, K., Yang, X., 2022. Water clarity mapping of global lakes using a novel hybrid deep-learning-based recurrent model with Landsat OLI images. *Water Res.* 215, 118241.
- Heiskanen, J., Mammarella, I., Ojala, A., Stepanenko, V., Erkkilä, K., Miettinen, H., Sandström, H., Eugster, W., Leppäranta, M., Järvinen, H., Vesala, T., Nordbo, A., 2015. Effects of water clarity on lake stratification and lake-atmosphere heat exchange. *J. Geophys. Res. Atmos.* 120 (15), 7412–7428.
- Hocking, G.C., Straškraba, M., 1999. The effect of light extinction on thermal stratification in reservoirs and lakes. *Int. Rev. Hydrobiol.* 84 (6), 535–556.
- Huang, A., Lazhu Wang, J., Dai, Y., Yang, K., Wei, N., Wen, L., Wu, Y., Zhu, X., Zhang, X., Cai, S., 2019. Evaluating and improving the performance of three 1-d Lake models in a large deep lake of the central Tibetan plateau. *J. Geophys. Res. Atmos.* 124 (6), 3143–3167.
- Li, Y., Zhang, Q., Liu, X., Yao, J., 2020. Water balance and flashiness for a large floodplain system: a case study of Poyang Lake, China. *Sci. Total Environ.* 710, 135499.
- Lv, Z., Zhang, S., Jin, J., Wu, Y., Ek, M.B., 2019. Coupling of a physically based lake model into the climate forecast system to improve winter climate forecasts for the Great Lakes region. *Clim. Dynam.* 53, 6503–6517.
- McCullough, I.M., Loftin, C.S., Sader, S.A., 2012. Combining lake and watershed characteristics with Landsat TM data for remote estimation of regional lake clarity. *Rem. Sens. Environ.* 123, 109–115.
- McPherson, M.L., Hill, V.J., Zimmerman, R.C., Dierssen, H.M., 2011. The optical properties of greater Florida bay: implications for seagrass abundance. *Estuar. Coast* 34 (6), 1150–1160.
- Mironov, D.V., 2008. Parameterization of Lakes in Numerical Weather Prediction. Description of a lake Model, COSMO Technical Report, No. 11. Deutscher Wetterdienst, Offenbach am Main, Germany, p. 41pp.
- Oleson, K., Lawrence, D., Bonan, G., Drewniak, B., Huang, M., Koven, C., Levis, S., Li, F., Riley, W., Subin, Z., 2013. Technical Description of Version 4.5 of the Community Land Model (CLM), NCAR Technical Note: NCAR/TN-503+ STR. National Center for Atmospheric Research (NCAR), Boulder, CO, USA.
- Olmanson, L.G., Brezonik, P.L., Bauer, M.E., 2013. Geospatial and temporal analysis of a 20-year record of landsat-based water clarity in Minnesota's 10,000 lakes. *JAWRA J. American Water Resources Associat.* 50 (3), 748–761.

- O'reilly, C.M., Sharma, S., Gray, D.K., Hampton, S.E., Read, J.S., Rowley, R.J., Schneider, P., Lenters, J.D., Mcintyre, P.B., Kraemer, B.M., Weyhenmeyer, G.A., Straile, D., Dong, B., Adrian, R., Allan, M.G., Anneville, O., Arvola, L., Austin, J., Bailey, J.L., Baron, J.S., Brookes, J.D., De Eyto, E., Dokulil, M.T., Hamilton, D.P., Havens, K., Hetherington, A.L., Higgins, S.N., Hook, S., Izmet'eva, L.R., Joehnk, K.D., Kangur, K., Kasprzak, P., Kumagai, M., Kuusisto, E., Leshkevich, G., Livingstone, D.M., Macintyre, S., May, L., Melack, J.M., Mueller-Navarra, D.C., Naumenko, M., Noges, P., Noges, T., North, R.P., Plisnier, P.D., Rigosi, A., Rimmer, A., Rogora, M., Rudstam, L.G., Rusak, J.A., Salmaso, N., Samal, N.R., Schindler, D.E., Schladow, S.G., Schmid, M., Schmidt, S.R., Silow, E., Soylu, M.E., Teubner, K., Verburg, P., Voutilainen, A., Watkinson, A., Williamson, C.E., Zhang, G.Q., 2015. Rapid and highly variable warming of lake surface waters around the globe. *Geophys. Res. Lett.* 42 (24), 10773–10781.
- Padiál, A., Thomaz, S., 2008. Prediction of the light attenuation coefficient through the Secchi disk depth: empirical 269 modeling in two large Neotropical ecosystems. *Limnology* 9 (2), 143–151.
- Poole, H., Atkins, W., 1929. Photo-electric measurements of submarine illumination throughout the year. *J. Marine Biol. Assoc. UK* 16 (1), 297–324.
- Potes, M., Costa, M.J., Salgado, R., 2012. Satellite remote sensing of water turbidity in Alqueva reservoir and implications on lake modelling. *Hydrol. Earth Syst. Sci.* 16 (6), 1623–1633.
- Qi, L.Y., Huang, J.C., Huang, Q., Gao, J.F., Wang, S.G., Guo, Y.Y., 2018. Assessing aquatic ecological health for lake Poyang, China: Part I index development. *Water* 10 (7), 943.
- Rinke, K., Yeates, P.S., Rothhaupt, K.-O., 2010. A simulation study of the feedback of phytoplankton on thermal structure via light extinction. *Freshw. Biol.* 55 (8), 1674–1693.
- Samuelsson, P., Kourzeneva, E., Mironov, D., 2010. The impact of lakes on the European climate as simulated by a regional climate model. *Boreal Environ. Res.* 15 (2), 113–129. <http://hdl.handle.net/10138/233079>.
- Shang, S., Lee, Z., Shi, L., Lin, G., Wei, G., Li, X., 2016. Changes in water clarity of the bohai sea: observations from MODIS. *Rem. Sens. Environ.* 186, 22–31.
- Shankman, D., Keim, B.D., Song, J., 2006. Flood frequency in China's Poyang Lake region: trends and teleconnections. *Int. J. Climatol.* 26 (9), 1255–1266.
- Shatwell, T., Thiery, W., Kirillin, G., 2019. Future projections of temperature and mixing regime of European temperate lakes. *Hydrol. Earth Syst. Sci.* 23 (3), 1533–1551.
- Shimoda, Y., Azim, M.E., Perhar, G., Ramin, M., Kenney, M.A., Sadraddini, S., Gudimov, A., Arhonditsisa, G.B., 2011. Our current understanding of lake ecosystem response to climate change: what have we really learned from the north temperate deep lakes? *J. Great Lake. Res.* 37 (1), 173–193.
- Stepanenko, V.M., Machulskaya, E., Glagolev, M.V., Lykossov, V.N., 2012. Numerical modeling of methane emissions from lakes in the permafrost zone. *Izvestiya Atmos. Ocean. Phys.* 47 (2), 252–264.
- Subin, Z.M., Riley, W.J., Mironov, D., 2012. An improved lake model for climate simulations: model structure, evaluation, and sensitivity analyses in CESM1. *J. Adv. Model. Earth Syst.* 4, M02001.
- Thiery, W., Davin, E.L., Panitz, H.-J., Demuzere, M., Lhermitte, S., Lipzig, N. van., 2015. The impact of the african great lakes on the regional climate. *J. Clim.* 28 (10), 4061–4085.
- Thiery, W., Stepanenko, V.M., Fang, X., Johnk, K.D., Li, Z.S., Martynov, A., Perroud, M., Subin, Z.M., Darchambeau, F., Mironov, D., Van Lipzig, N.P.M., 2014. LakeMIP Kivu: evaluating the representation of a large, deep tropical lake by a set of one-dimensional lake models. *Tellus Dyn. Meteorol. Oceanogr.* 66 (1), 1–12.
- Tian, L., Jin, J., Wu, P., Niu, G., Zhao, C., 2020. High-resolution simulations of mean and extreme precipitation with WRF for the soil-erosive Loess Plateau. *Clim. Dynam.* 54 (7–8), 3489–3506.
- Wang, F., Li, Q., Wang, Y., 2020a. Lake-atmosphere exchange impacts ozone simulation around a large shallow lake with large cities. *Atmos. Environ.* 246, 118086.
- Wang, S., Li, J., Zhang, B., Lee, Z., Spyros, E., Feng, L., Liu, C., Zhao, H., Wu, Y., Zhu, L., Jia, L., Wan, W., Zhang, F., Shen, Q., Tyler, A.N., Zhang, X., 2020b. Changes of water clarity in large lakes and reservoirs across China observed from long-term MODIS. *Rem. Sens. Environ.* 247, 111949.
- Woolway, R.I., Jennings, E., Shatwell, T., Golub, M., Pierson, D.C., Maberly, S.C., 2021. Lake heatwaves under climate change. *Nature* 589 (7842), 402–407.
- Woolway, R.I., Merchant, C.J., 2019. Worldwide alteration of lake mixing regimes in response to climate change. *Nat. Geosci.* 12 (4), 271–276.
- Wu, Y., Huang, A., Yang, B., Dong, G., Wen, L., Lazhu Zhang, Z., Fu, Z., Zhu, X., Zhang, X., Cai, S., 2019. Numerical study on the climatic effect of the lake clusters over Tibetan Plateau in summer. *Clim. Dynam.* 53 (6part2), 5215–5236.
- Wu, Z.S., Zhang, D.W., Cai, Y.J., Wang, X.L., Zhang, L., Chen, Y.W., 2017. Water quality assessment based on the water quality index method in Lake Poyang: the largest freshwater lake in China. *Sci. Rep.* 7 (1), 17999.
- Xu, L., Liu, H., Du, Q., Wang, L., 2016. Evaluation of the WRF-lake model over a highland freshwater lake in southwest China. *J. Geophys. Res. Atmos.* 121 (23), 13989–14005.
- Yu, Z., Yang, K., Luo, Y., Shang, C., Zhu, Y., 2020. Lake surface water temperature prediction and changing characteristics analysis - a case study of 11 natural lakes in Yunnan-Guizhou Plateau. *J. Clean. Prod.* 276, 122689.
- Zhang, G., Yao, T., Xie, H., Qin, J., Ye, Q., Dai, Y., Guo, R., 2014. Estimating surface temperature changes of lakes in the Tibetan Plateau using MODIS LST data. *J. Geophys. Res. Atmos.* 119 (14), 8552–8567.
- Zhang, G., Duan, S., 2021. Lakes as sentinels of climate change on the Tibetan Plateau. *All Earth* 33 (1), 161–165.
- Zhang, Q., Jin, J., Wang, X., Budy, P., Null, S.E., 2019. Improving lake mixing process simulations in the community land model by using k profile parameterization. *Hydrol. Earth Syst. Sci.* 23 (12), 4969–4982.
- Zhang, Y., Liu, X., Yin, Y., Wang, M., Qin, B., 2012. Predicting the light attenuation coefficient through Secchi disk depth and beam attenuation coefficient in a large, shallow, freshwater lake. *Hydrobiologia* 693 (1), 29–37.
- Zhang, Y., Qin, B., Shi, K., Zhang, Y., Deng, J., Wild, M., Li, L., Zhou, Y., Yao, X., Liu, M., Zhu, G., Zhang, L., Gu, B., Brookes, J.D., 2020. Radiation dimming and decreasing water clarity fuel underwater darkening in lakes. *Sci. Bull.* 65 (19), 1675–1684.
- Zhao, J., Li, L., Li, J., Zhao, R., Liu, X., Yang, J., 2019. The analysis on the response of the water level change trend to human activities in Poyang lake (in Chinese abstract). *J. Jiangxi Normal Univ. (Natural Sci.)* 43 (5), 532–544.
- Zhu, L., Jin, J., Liu, Y., 2020. Modeling the effects of lakes in the Tibetan plateau on diurnal variations of regional climate and their seasonality. *J. Hydrometeorol.* 21 (11), 2523–2536.
- Zhen, L., Li, F., Huang, H., Dilly, O., Liu, J., Wei, Y., Yang, L., Cao, X., 2011. Households' willingness to reduce pollution threats in the Poyang Lake region, southern China. *J. Geochem. Explor.* 110 (1), 15–22.
- Zolfaghari, K., Duguay, C.R., Pour, H.K., 2017. Satellite-derived light extinction coefficient and its impact on thermal structure simulations in a 1-D lake model. *Hydrol. Earth Syst. Sci.* 21 (1), 377–391.